AIAA SciTech Forum
6-10 January 2020, Orlando, FL
AIAA Scitech 2020 Forum

10.2514/6.2020-1887

Controlled electric charging of an aircraft in flight using corona discharge

Carmen Guerra-Garcia*
Massachusetts Institute of Technology (MIT), Cambridge, MA, 02139, USA

Pol Fontanes†, Michele Urbani‡, Joan Montanya§
Universitat Politècnica de Catalunya (UPC), Terrassa, Barcelona, Spain

Theodore Mouratidis¶, Manuel Martinez-Sanchez‖ and Ngoc Cuong Nguyen**
Massachusetts Institute of Technology (MIT), Cambridge, MA, 02139, USA

This work is part of an ongoing study to provide an artificial means of controlling the net electrical charge of an aircraft in flight through charge emission. The charging system consists on an onboard d.c. high voltage power supply (of the order of 10 kV) with the high voltage terminal connected to a coronating anode and the low voltage terminal connected to the body whose potential needs to be controlled. The system must be electrically floating and exposed to wind. During an initial transient, the positive ions produced by the corona are convected away by the wind and the body charges negatively in response. This paper presents a theoretical model of the charging strategy that reveals two distinct regimes of charging and corona operation, as well as wind tunnel experiments using both a sphere-corona tip assembly and a 2D wing-corona wire assembly that confirm the theoretical predictions. Finally, we implement the system in an RC aircraft to demonstrate that charging in flight using corona discharge is feasible and does not affect flight operations.

I. Introduction

Aircraft get electrically charged during takeoff and flight. First, in the presence of ambient electric fields, even neutrally charged aircraft become polarized, with one end becoming negatively charged and the other positively charged [1]. This is true both for metallic and composite structures, since metallic mesh or foil is embedded in composite frames to ensure a fully conductive path in the event of a lightning strike. In addition, aircraft acquire net charge from a number of sources including: corona discharge appearing at the sharp extremities of the vehicle, contact electrification between the wheels and the runway during take-off, charged particles coming out of the engine exhaust, and through collisions with charged precipitation, aerosol particles or dust in the atmosphere [2]. Natural charging mechanisms can lead to significant net charging levels, of the order of 0.1-1 mC [3]. Considering a self-capacitance of 1000 pF, this translates into electric potentials of 0.1-1 MV with respect to the environment.

A handful of studies have explored the possibility of artificially charging aircraft using charge emission from the surface using either ions [3] or charged water droplets [4, 5]; and with different objectives in mind. In their 1946 paper, Stimmel [5] and Waddel [4] artificially charged a B-17 research airplane using charged water droplet emission, with the goal of simulating autogenous charging of an airplane in any weather. In this work, they claim to reach a potential of about 0.5 MV, which translates to a net charge of 0.4 mC given the self-capacitance of 780 pF. Since this level is of the same order of magnitude as the natural charging levels encountered during flight, the system was able to counteract any autogenous charging, but was not considered a practical solution due to the considerable bulk and weight of the artificial charging system.

Artificial charging using a corona discharge was pursued in Ref. [3] using the Special Purpose Test Vehicle for Atmospheric Research (SPTVAR), which is a modified Schweizer 845 airframe fitted with a turbocharged engine. The

*Boeing Assistant Professor, Aeronautics and Astronautics, AIAA Senior Member. guerrac@mit.edu
†Graduate Research Assistant, Department of Electrical Engineering; and Visiting Student at MIT.
‡Graduate Research Assistant, Department of Electrical Engineering; and Visiting Student at MIT.
§Professor, Department of Electrical Engineering.
¶Graduate Research Assistant, Aeronautics and Astronautics.
‖Post-tenure Professor, Aeronautics and Astronautics, AIAA Senior Member.
**Research Scientist, Aeronautics and Astronautics, AIAA Member.

artificial charging system consisted on a high-voltage stinger probe that uses an onboard high-voltage power supply (of the order of 1-10 kV), with the high voltage terminal connected to a point or brush that produces a corona discharge exposed to the airstream. The low voltage terminal was connected to the airframe of which the potential was to be controlled. In these experiments, the objective was to use the charging system to calibrate a series of electric field mills onboard used to measure ambient electric fields, and compensate for the aircraft's net charge. The charging levels in this case were lower, of the order of 20-40 μC, most likely due to the higher electrical mobility of ions as compared to heavier droplets although the physical mechanisms of charging were not described in detail. The study focused on a proof of concept demonstrating on/off operation.

Artificial electric potential compensation of the order of 40 kV has also been pursued for helicopters, with the objective of minimizing charging of heavy-lift vehicles, for safety reasons [6]. In this case, the charging currents coming out from the exhaust were modified by electrostatic shielding of the engine's exhaust and applying controllable electric fields.

We have recently proposed that the net charge of an aircraft in flight affects its risk of being struck by lightning [7] and that artificially charging the vehicle could be used as a means to reduce the probability of lightning initiation by aircraft [1, 8]. More specifically, aircraft trigger lightning through a bi-directional leader process that is initiated by the aircraft. Typically the positive leader precedes since the breakdown threshold is lower for the positive polarity than for the negative polarity; so a negative charging level that equalizes both critical fields would be preferred in terms of lightning avoidance. We have recently demonstrated this hypothesis in a long arc laboratory experiment [9] that confirms that the positive leader is triggered at higher ambient fields, if the vehicle is negatively charged (up to a certain level at which the negative leader becomes more likely). The experiment showed that the breakdown field could vary by as much as 30% for the range of charging levels tested (up to 40 kV negative, and using a model aircraft with a 1 m wingspan), in accordance with our prior theoretical work [1].

This paper gives a comprehensive overview of our ongoing efforts to achieve controlled electrical charging of an aircraft in flight, that include theory, laboratory experiments and field campaigns. The paper is organized as follows. Section II summarizes the theory of charging of an isolated flying body by corona discharge [10]. Section III describes wind tunnel campaigns in the MIT Wright Brothers Wind Tunnel to demonstrate artificial charging by corona discharge of an electrically isolated sphere, followed by experiments with an electrically isolated 1 m-span wing exposed to winds of up to 50 m/s [10, 11]. Section IV describes the first results from a flight campaign planned to demonstrate these ideas in flight. Finally, section V summarizes the main findings of our work and outlines the next steps.

II. Theory of charging by corona discharge

A. Formulation

In order to charge a floating body to negative levels, positive charge has to be emitted from the surface. In the strategy considered, positive ions formed in the vicinity of a coronating anode are convected away by the wind, charging the body that serves as the floating cathode to negative values in response. In order to facilitate the evacuation of positive charge, we seek the glow corona regime, in which electrons / positive ion pairs are produced in close proximity to the electrode so that electrons are rapidly absorbed by the anode and the field is too high for significant attachment to take place. Hence, a positive ion cloud is generated which will be affected by the influence of the wind as well as the electrostatic attraction to the floating cathode.

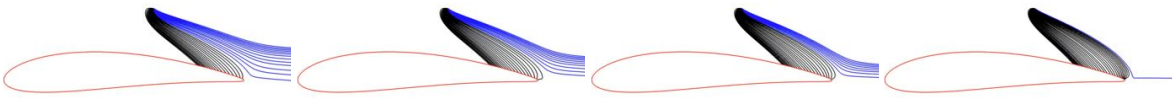

Fig. 1 Ion streamlines for corona wire/ wing configuration during the transient charging phase (left to right). Result from simulation. Blue corresponds to ions that escape, carried away by the wind; black corresponds to ions that are attracted by the charged wing. As the wing becomes more negative, more ions are attracted to it until in steady state all of the ions return and the wing has settled to the final potential value (last image).

To study the potential and limitations of this charging strategy we selected a 2D wing-wire configuration, where the body to be charged is a wing and the coronating electrode is a small diameter wire placed in the rear side of the airfoil to

facilitate positive ion evacuation, Figure 1. To solve for the transport of ions under these conditions, we solve the steady state current conservation equation accounting for ion current alone, and as influenced by the electrostatic attraction and the wind, along with the Poisson equation to track the evolution of the space charge cloud. The wind velocity field around wing and wire is numerically calculated assuming potential flow solution. This system of equations can be solved non-dimensionally choosing the following variables as reference: the breakdown value for atmospheric pressure air, E_0, for the electric field; the ion drift velocity under breakdown conditions, $\mu_i E_0$, for the velocity; the wire radius, a, for the length scale; and $\epsilon_0 E_0/a$ for the ion charge density.

The boundary conditions on the electrostatic potential are the values at the wing and at the wire (which is the wing value plus the power supply bias), normalized by $E_0 a$. The wing potential is however an unknown a priori since the wing gets charged by the corona discharge. In order to solve for the wing potential value, we follow an iterative procedure: initially the wing is unbiased, as the corona is turned on some ions are convected away and the wing charges negatively in response. As the wing gets more negative, a larger fraction of the ions are attracted back to the wing, which continues to charge negatively as long as a fraction of the ions is convected away. This iterative procedure is continued until all of the ions are attracted back to the wing: this is the potential at which the wing settles, see Figure 1. The boundary condition on the wire surface is an ion emission condition based on the Peek formulation [12, 13]. Note that this boundary condition can not be completely formulated in non-dimensional form because the Peek field for a cylindrical wire depends on its radius:

$$E_P/E_0 = 1 + \frac{0.0308}{\sqrt{a[m]}}, \tag{1}$$

and so the value for $a = 0.1mm$, as used in all the experiments reported in this paper, is used.

Details of the numerical solution method are reported in [14].

B. Model results and discussion

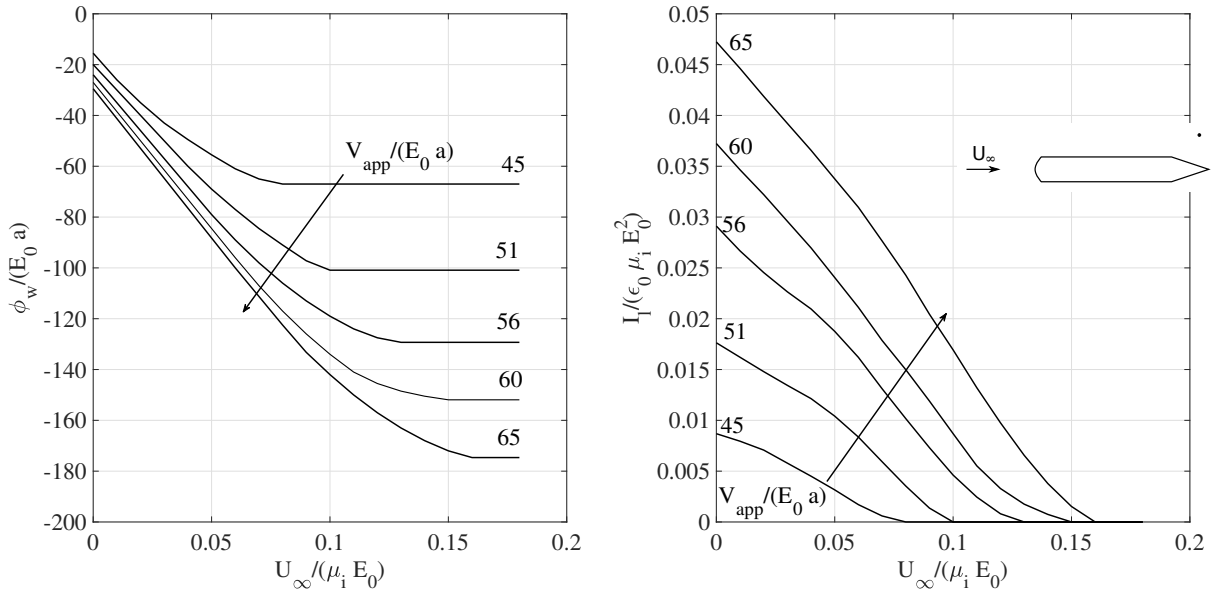

Fig. 2 Charging of wing by glow corona discharge and corona current (per unit length) as a function of wind speed and power supply bias for same geometry as in section III.C. Results from model.

The charging and corona current per unit length predicted by the model, for the geometry of the experiment reported in section III.C and shown in the insert of the graph, is plotted in Figure 2. Two regimes are found. The first one, at low wind speeds and for fixed power supply bias, leads to increased charging with wind speed: the potential of the wing becomes more negative as the wind speed increases. This is accompanied by a decreases in the corona current, which is unintuitive because it is the opposite trend to what has been reported before [15, 16]. The explanation for this trend

is that as the wind speed increases, the ion cloud gets dispersed and so the space charge shielding should be reduced (this effect tends to increase the current), however, the wing-wire system also becomes more negative with respect to the environment acting to suppress the positive corona (this effect tends to decrease the current). For the choice of wing-wire position reported in this paper the second effect dominates and the current decreases with the wind speed. The second regime appears when the excursion to negative potentials is so high that the positive corona can no longer be sustained and the current goes to zero. The potential then saturates and can no longer be decreased by further increasing the wind speed. In order to further decrease the wing potential, the power supply bias can be increased. The model assumes there are no other charging/ discharging mechanisms present aside from the current emission by the wire.

Note that even though we chose to plot the results in non-dimensional units, the geometry selected plays an important role and different geometries and wing/wire placements lead to different charging curves. There is actually an optimum position of the wire that maximizes charging (section III.B).

III. Wind tunnel campaigns

A. Experimental setup

Wind tunnel tests were used to demonstrate the feasibility of electrically charging a floating object using corona discharge exposed to high winds and validating the theoretical results summarized in Section II. A diagram and photographs of the experimental setup are shown in Figure 3. The experiments with the wing-corona wire assembly were performed in the MIT Wright Brothers Wind Tunnel, that has an elliptical cross section of 3 m x 2.3 m and achieves wind speeds of up to 60 m/s. The experiments with the sphere-corona tips assembly here reported were performed in a 0.46 m x 0.46 m open section wind tunnel with a top speed of 40 m/s.

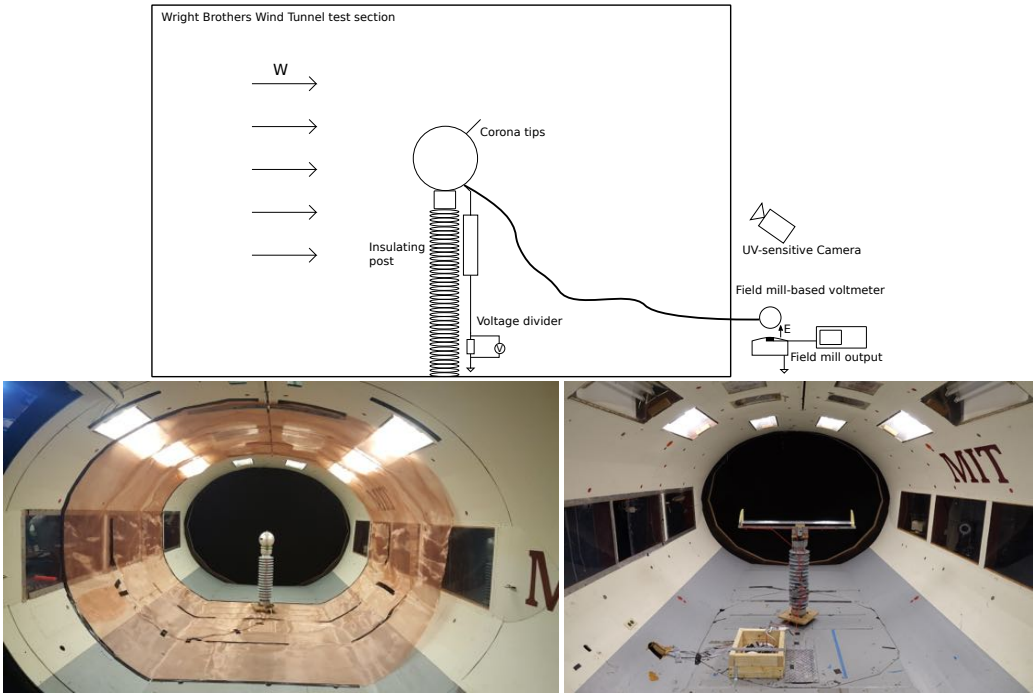

Fig. 3 Wind tunnel experimental setup. (Top) schematic of experimental assembly inside the wind tunnel; (bottom left) photograph of sphere-corona tip assembly; (bottom right) photograph of wing-corona wire assembly.

The first configuration tested used a metallic sphere of 10 cm radius to represent the body to be artificially biased. The coronating electrode was a bundle of six tungsten wires connected to the high voltage terminal of a floating high voltage power supply (EMCO Model E121, d.c. voltage up to 12 kV) powered by batteries. The low voltage terminal of the power supply was connected to the sphere. A spherical geometry was selected to place the electronics inside the sphere, and the electronics were operated remotely using an RF switch.

The second configuration tested was a 1 m span metallic wing with a 14 cm chord, 2 cm thick symmetric airfoil with

a 0.2 mm diameter corona wire placed parallel to the trailing edge of the airfoil (different positions of the wire were tested). The geometry of the setup is shown in the insert of Figure 2. In this case, the electronics had to be placed outside of the body to be charged, and they were located on the floor of the wind tunnel inside a copper nest electrically isolated by teflon blocks. Since the electronics could be slightly larger in these experiments, the floating power supply used was a Matsusada RB60-30P which could deliver up to 20 kV d.c. and was again operated remotely.

Both configurations (sphere-corona tip assembly and wing-corona wire assembly) were tested at wind speeds from 0-50 m/s. The assembly was mounted on top of a corrugated ceramic post of 1 m length electrically rated to withstand voltage differences of up to 70 kV to ensure electrical isolation from the environment. For some of the tests the wind tunnel walls were covered by copper mesh to avoid charging of the walls.

Diagnostics used included measurement of the negative potential achieved by the body-coronating electrode assembly by contact and non-contact measurements. The contact measurement consisted on a high voltage divider with 10 GΩ and 10 MΩ resistors in series. The non-contact measurement used an electric field mill mounted flush on a metal bowl placed 20 cm away from a second metallic sphere of smaller diameter and electrically connected to the sphere whose potential we wanted to measure. This setup ensured that both spheres were at the same potential and by measuring the potential of the small sphere using a calibrated electric field mill we could measure the floating potential of our assembly. The field mill based voltmeter was physically placed outside of the wind tunnel, Figure 3. The calibration of the electric field mill was done by charging the second sphere using a high voltage power supply and under the same environment in which data was to be collected. In addition, the current of the corona was measured by monitoring the current from the onboard power supply and UV imaging of the corona discharge was obtained using a CoronaFinder mounted on a digital camera video recording at 30 frames per second.

B. Results with sphere-corona tip assembly

Initial charging experiments were planned with a spherical body and a bundle of six corona points aligned 45 degrees to the incoming flow and on the downstream side of the sphere (Figure 3) with variable length of the protruding bundle. Two configurations were tested with the tips together and splayed to reduce space charge effects between tips.

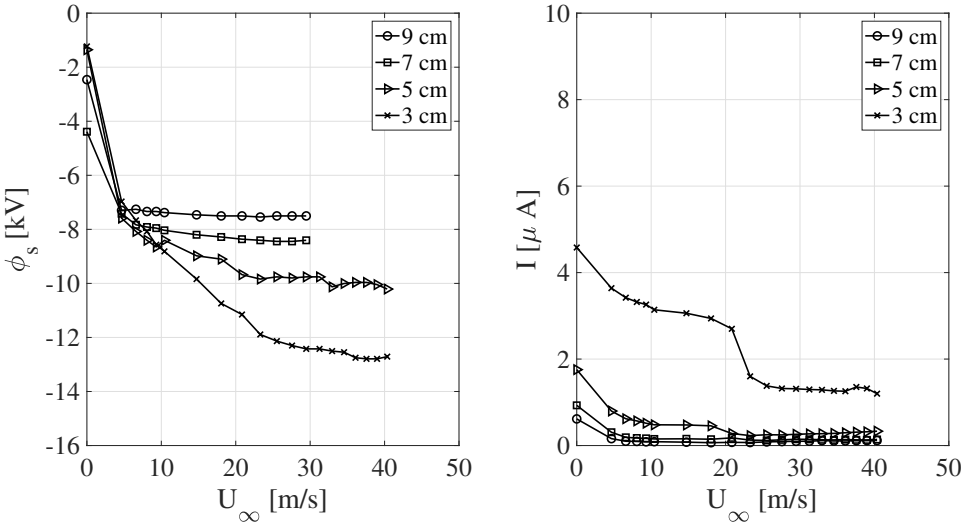

Fig. 4 Charging of sphere by corona discharge and corona current as a function of wind speed for fixed power supply bias of 11kV. Experimental results for bundled tips, different lengths of protruding bundle.

Figures 4 and 5 summarize the results. For both configurations, current decreases with wind and the sphere potential goes to more negative values as wind increases up to a saturation value, indicating that the excursion of the sphere-corona tip assembly to negative potentials with respect to the environment leads to a weakening of the corona and that this effect dominates over the dispersion of the ion cloud by the wind.

In the case of tips in a bundle (Figure 4), it is interesting to note the discrete step reduction in the current (e.g. around 20 m/s for the 3 cm length configuration). Visually, this corresponded with individual corona tips turning off as the system became more negative. For the bundled tips, space charge effects were so strong that only a few tips were

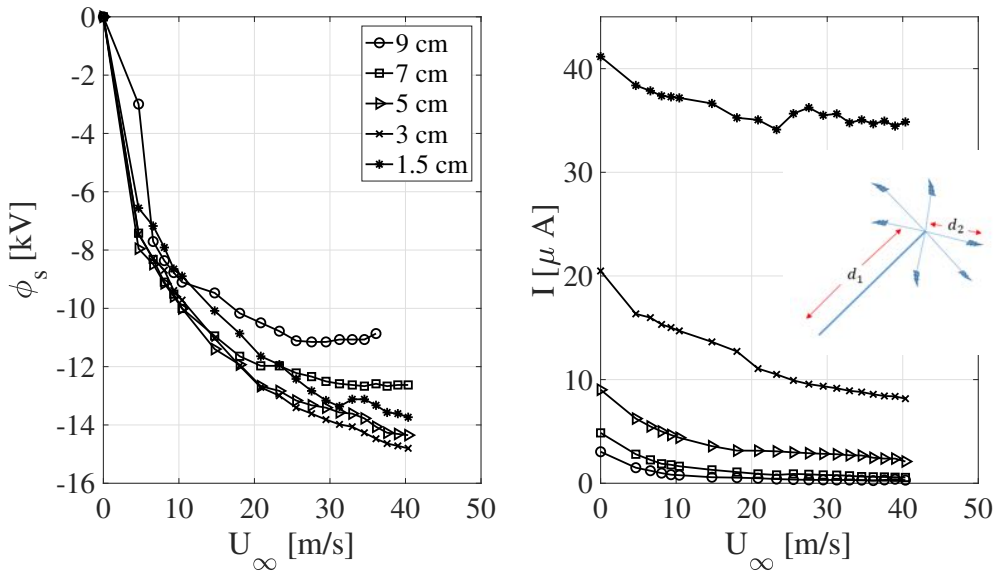

Fig. 5 Charging of sphere by corona discharge and corona current as a function of wind speed for fixed power supply bias of 11kV. Experimental results for splayed tips, different lengths of protruding bundle d_1, d_2= 6 cm.

emitting at a time, thus the low currents observed. In addition, there is a strong effect of the length of the protruding bundle on both the current emitted and the potential achieved. On the one hand, the shorter the bundle, the stronger the corona (since the field is enhanced by the proximity of the cathode), but also the greater the electrostatic attraction of the positive ions to the sphere. In the cases shown, the first effect dominates and so shorter bundles lead to both higher current and higher charging.

When moving to the splayed tip configuration (Figure 5), space charge effects between tips were significantly reduced and mostly all of the tips were emitting simultaneously, Figure 6. This led to comparatively higher corona current and more charging. The strong effect of the position of the corona tips relative to the sphere is again observed. For the shorter bundle tested, although the corona current is largest, the charging is limited due to the strong attraction of the ions to the sphere. There is therefore an optimum position of the corona bundle for charging, in this case between 1.5 and 3 cm.

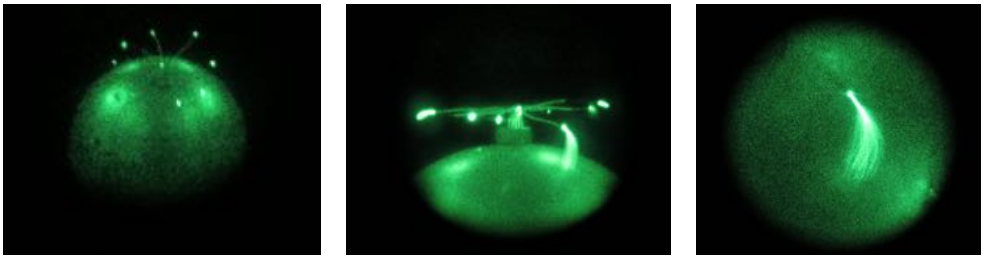

Fig. 6 UV photographs of corona discharges from 8 splayed tips showing streamer features. Note the experiments reported were performed with 6 tips in an equivalent configuration.

The theoretical analysis of this configuration is more challenging than the wire-wing assembly, not only because of the flow structure in the downstream section of the sphere, but also the 3D effects that can not be bypassed and the nature of the corona discharge which was most of the time in the streamer regime, as seen in Figure 6. Nevertheless charging is possible in this regime and similar trends as those seen using the glow regime reported in section III.C are observed.

C. Results with wing-corona wire assembly

According to the model results in section II, for an applied voltage of $V_{app} = 45E_0a$, the wing should charge to $\phi_w = -67E_0a$ and the saturation velocity is $U_\infty = 0.08\mu_i E_0$ (Figure 2). Using $a = 0.1mm$ and $E_0 = 2.9kV/mm$, this translates to charging to almost -20 kV using a 13 kV bias of the power supply. For an ion mobility of about $\mu_i = 1.5 \cdot 10^{-4} m^2 V^{-1} s^{-1}$, saturation of the potential would occur at around 35 m/s. Experiments were performed at different voltage levels of the power supply which corroborated the theoretical model results. Figure 7 shows the experimental data (non-dimensionalized) overlapped with the theoretical curves, they are in excellent agreement confirming the existence of the two regimes: increased charging with wind speed up to a saturation level at which the corona becomes very weak. A characteristic photograph of the discharge taken with the UV camera is presented as an insert to the graph. It is clear that the discharge observed is of the glow corona type.

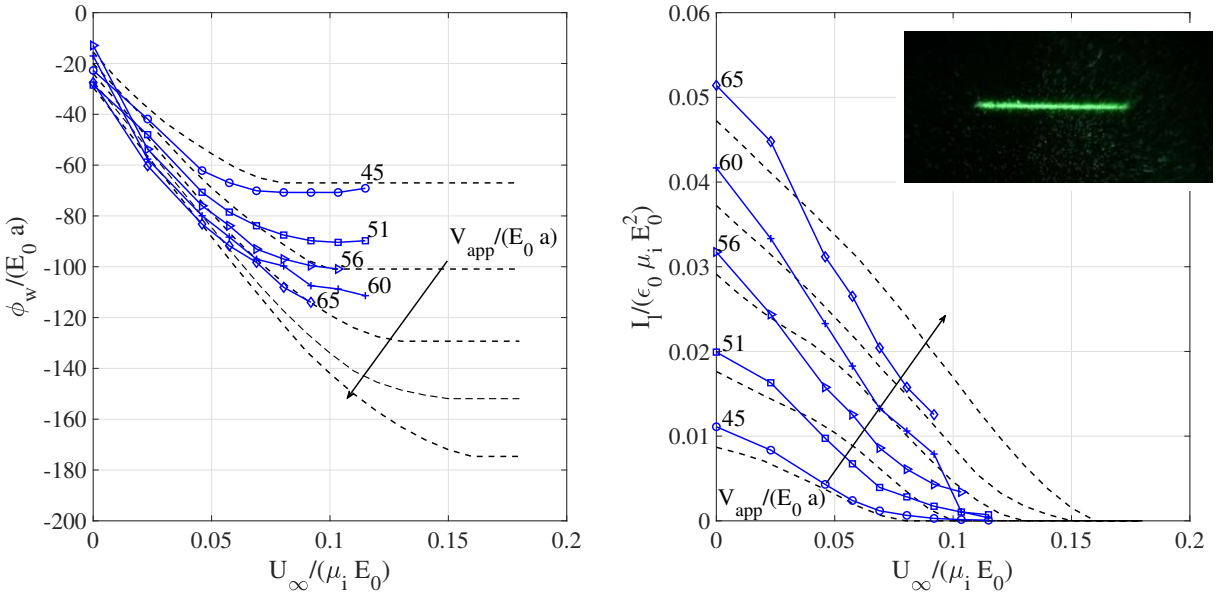

Fig. 7 Charging of wing by glow corona discharge and corona current (per unit length) as a function of wind speed and power supply bias. Experimental results superimposed to theoretical curves.

IV. Proof-of-concept flight campaign

Our current efforts are focused on developing a UAV platform to demonstrate charge control in flight and during fair weather conditions. This is an ongoing effort of which the first successful flight is reported in this paper.

A. Airborne platform

The first iteration of this experiment uses an off-the-shelf electric RC aircraft (Multiplex Easycub*) with a 1.4 m wingspan and 1 m long fuselage. The plane is fitted with a 1.2 m corona wire parallel to the wing and an onboard high voltage power supply (Ultravolt 15 A, 5-15 kV d.c.), with the high voltage terminal connected to the wire and the low voltage terminal connected to the fuselage. The fuselage was spray painted with electrically conductive paint to ensure electrical conductivity in order to avoid differential charging and demonstrate net charge control. An electric field mill (EFM 113B) is carried onboard to infer the net charge of the vehicle when the corona emitter is turned on. The calibration of the single electric field mill to measure the vehicle's net charge assumes a negligible contribution of the ambient electric field. The vehicle is RC controlled and telemetry for data transmission (relative wind velocity measured by a pitot probe, corona current and EFM measurement) and power supply voltage control are incorporated. A photograph of the vehicle fitted with the corona wire and sensors is shown in Figure 8.

*https://hitecrcd.com/products/airplanes/multiplex/easy-cub-rr/product

Fig. 8 RC aircraft fitted with corona wire along wingspan, pitot tube in vertical stabilizer, EFM mounted flush to the surface, and spray painted with conductive paint.

This proof-of-concept flight had the objective to demonstrate ability to electrically charge a fixed-wing, conductive aircraft during flight and fair-weather conditions, using corona discharge, to levels that (i) would have a measurable effect on lightning initiation and (ii) are comparable to those achieved in the wind tunnel at the same speed.

B. Flight results

The results here reported were obtained in Solsona, Lleida, Spain on August 9, 2019. The plane performed a 7 minute duration flight during which the onboard power supply bias was varied from zero to 12 kV and data of current emitted and voltage reached by the system was transmitted to ground. In addition, a pitot tube on board measured the wind speed. These tests were focused on feasibility of the strategy and future flights will gather data under different flight speeds and voltage levels, as well as study the charging and discharging rates. The flight data recorded during the first successful flight is shown in Figure 9. The blue lines show the control knobs of the experiment, i.e., the wind speed (dashed line) and the power supply bias (continuous line). The red lines show the performance of the corona-charging system. i.e., the plane potential achieved (top graph) and the corona current measured (bottom graph).

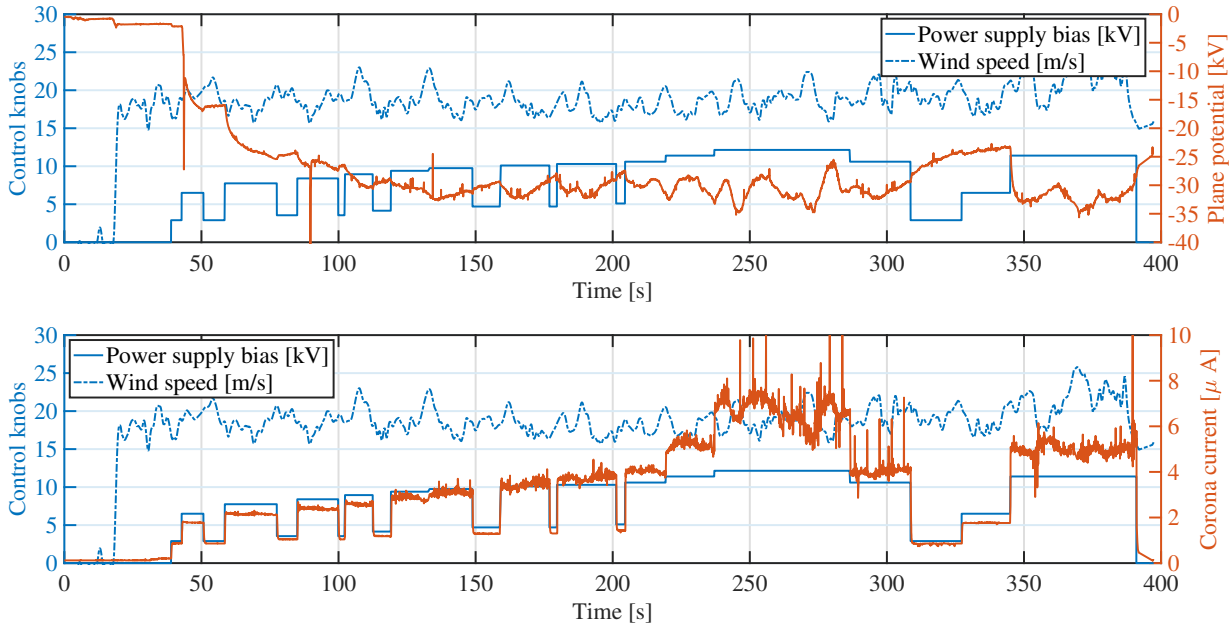

Fig. 9 Flight data recorded during 7 min flight. The plane potential and corona current are plotted as a function of time, for a flight speed of around 20 m/s and power supply bias varying between zero and 12 kV.

The following comments apply. The plane is hand-launched at about 18 s after start of data recording (as marked by

the sudden increase in the wind speed) at which time the high voltage power supply is turned off and the plane potential is close to zero. At 43 s, the power supply bias is increased to 6.5 kV, close to the corona inception threshold, and the plane charges to -16 kV. The power supply bias is incrementally increased (with alternate segments of voltage decrease, due to a failed communication with the onboard system), and the aircraft potential continues to decrease up to about -32 kV at 137 s (bias of 9.75 kV). This -32 kV limit could not be surpassed by further increasing the power supply bias, indicating that the airplane was probably generating spurious coronae at sharp edges (of negative polarity due to the negative charging) that could not be compensated by the current of the wire corona.

As the power supply bias is increased, the current emitted by the corona also increases. At the higher levels of the power supply bias tested, above 10.6 kV (between 245 s and 310 s), the sharp spikes in the current data indicate transition to the streamer regime and sparking. It is also worth noting the strong correlation between local excursions to more negative aircraft potentials and local increases in the wind speed. Although the trend is as expected (higher wind speed leads to more negative charging) at this point it is unclear if those fluctuations could be due to noise coupling between signals. Discharging features can be seen when the power supply bias is suddenly decreased below the corona inception threshold, e.g. at 309 s.

The results of Figure 9 are plotted in Figure 10 as a function of power supply bias and wind speed and using time as a parameter. For clarity, not all the voltage levels tested are plotted. Although these results are still preliminary, some important features can be observed. The plane potential increases (in magnitude) both with applied voltage and wind speed, and the current increases with applied voltage and decreases with wind speed, as observed in the wind tunnel (section III) and explained theoretically for conditions that favor charging (section II). The charging/ discharging transients can also be observed (tails of data points with plane potential values going from zero to about 25 kV in magnitude). Note that the range of wind speeds tested is small, hence the small dependency with wind speed.

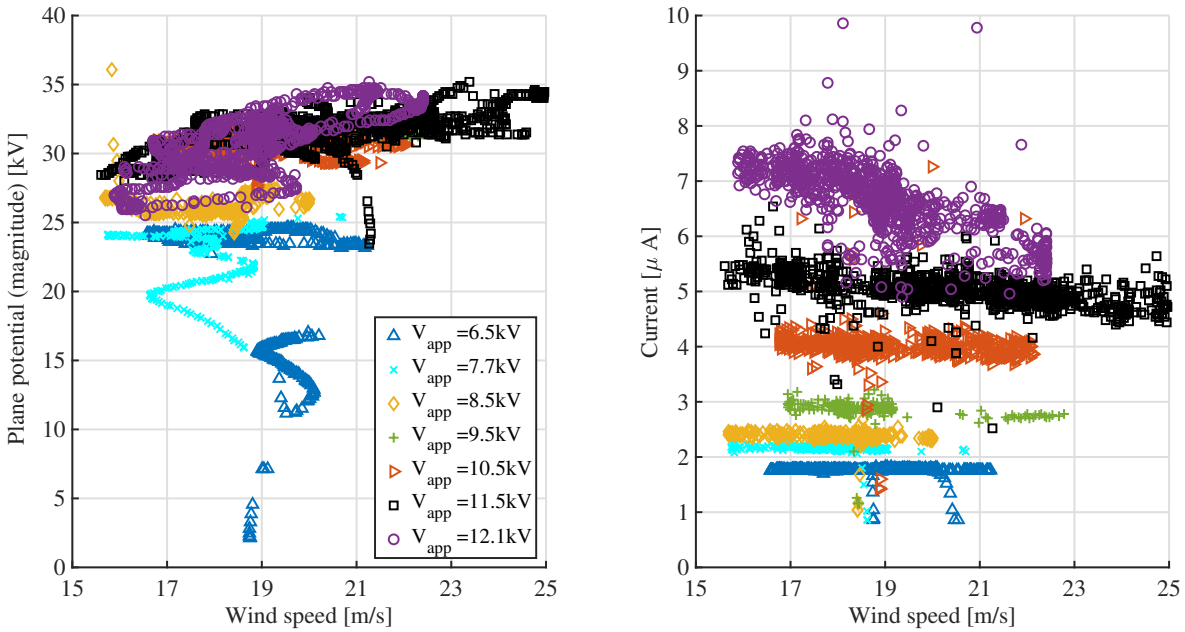

Fig. 10 Plane potential and corona current as a function of wind speed for a sample of power supply bias. Time as a parameter, same data as in Figure 9.

V. Conclusions

This paper gives a comprehensive overview of our efforts to develop a net charge control system for aircraft. The system consists on a high voltage d.c. power supply carried on board with the high voltage terminal connected to a coronating electrode and the low voltage terminal connected to the object whose potential needs to be controlled. We have presented a theoretical model of charging that reveals the competing effects between electrostatics and wind dispersion. The theoretical model is in excellent agreement with wind tunnel data taken with a 2D wing-wire assembly.

Experiments with a sphere-corona bundle configuration essentially show similar dependencies. Finally, we implement the system in an RC vehicle and demonstrate similar charging levels to those predicted theoretically and achieved in the wind tunnel. Current work is focused on the flight campaigns as well as other methods of charging.

Acknowledgments

This work was supported by The Boeing Company through the Strategic Universities for Boeing Research and Technology Program and the MIT-Spain La Caixa Foundation Seed Fund (MISTI Global Seed Funds grant program). The authors would like to thank J. Peraire (MIT) for useful discussions, D. Robertson (MIT) for operating the Wright Brothers Wind Tunnel, E. Garcia for piloting the RC aircraft, and O. van der Velde (U. Politècnica de Catalunya) for assistance during the flight.

References

[1] Guerra-Garcia, C., Nguyen, N. C., Peraire, J., and Martinez-Sanchez, M., "Charge control strategy for aircraft-triggered lightning strike risk reduction," *AIAA Journal*, Vol. 56, No. 5, 2018, pp. 1988–2002.

[2] Vonnegut, B., and Little, A. D., "Electrical behavior of an airplane in a thunderstorm," *Technical Report for Federal Aviation Agency*, 1965, pp. FAA–ADS–36.

[3] Jones, J. J., "Electric charge acquired by airplanes penetrating thunderstorms," *Journal of Geophysical research*, Vol. 95, No. D10, 1990, pp. 16589–16600.

[4] Waddel, R. C., Drutowski, R. C., and Blatt, W. N., "Army-navy precipitation-static project: Part II-aircraft instrumentation for precipitation-static research," *Proceedings of the IRE*, Vol. 34, No. 4, 1946, pp. 161–166.

[5] Stimmel, R. G., Rogers, E. H., Waterfall, F. E., and Gunn, R., "Army-navy precipitation-static project: Part III-Electrification of aircraft flying in precipitation areas," *Proceedings of the IRE*, Vol. 34, No. 4, 1946, pp. 167–177.

[6] Moore, C. B., Jones, J. J., Hunyady, S. J., Rison, W., and Winn, W. P., "Electrical hazards to airborne operations," Technical Report for The Applied Research and Technology Directorate ONR N00014-87-K-0783, 1991.

[7] Guerra-Garcia, C., Nguyen, N. C., Peraire, J., and Martinez-Sanchez, M., "Influence of net charge on the probability of lightning initiation from aircraft," *Proceedings of the 2017 International Conference on Lightning and Static Electricity (ICOLSE), Nagoya, Japan*, 2017.

[8] Martinez-Sanchez, M., Guerra-Garcia, C., Nguyen, N. C., Peraire, J., and Mouratidis, T., "Charge control system to reduce risk of an aircraft-initiated lightning strike," Massachusetts Institute of Technology, Cambridge, MA, U. S. Patent No. 10450086, 2019.

[9] Pavan, C., Fontanes, P., Urbani, M., Nguyen, N. C., Martinez-Sanchez, M., Peraire, J., Montanya, J., and Guerra-Garcia, C., "Aircraft Charging and its Influence on Triggered Lightning," *Submitted for publication*, 2019.

[10] Nguyen, N. C., Martinez-Sanchez, M., Mouratidis, T., Peraire, J., and Guerra-Garcia, C., "Charging of an Isolated Body by Glow Corona Discharge in a Wind Stream," *International Conference on Lightning and Static Electricity, Wichita, KS*, 2019.

[11] Mouratidis, T., "Aircraft Charging Using Ion Emission for Lightning Strike Mitigation: An Experimental Study," Master's thesis, Massachusetts Institute of Technology, Cambridge, MA, 2018.

[12] Mokrov, M. S., Raizer, Y. P., and Bazelyan, E. M., "Development of a positive corona from a long grounded wire in a growing thunderstorm field," *J. Phys. D: Appl. Phys.*, Vol. 46, 2013, p. 455202 (14pp).

[13] Peek, F. W., *Dielectric phenomena in High Voltage Engineering*, New York: McGraw Hill, 1929.

[14] Nguyen, N. C., Guerra-Garcia, C., Peraire, J., and Martinez-Sanchez, M., "Computational study of glow corona discharge in wind: biased conductor," *Journal of Electrostatics*, Vol. 89, 2017, pp. 1–12.

[15] Chapman, S., "Corona point current in wind," *Journal of Geophysical research*, Vol. 75, No. 12, 1970, pp. 2165–2169.

[16] Chapman, S., "The magnitude of corona point discharge current," *Journal of the Atmospheric Sciences*, Vol. 34, 1977, pp. 1801–1809.